Editors' Suggestion

Asymptotic safety guaranteed for strongly coupled gauge theories

Andrew D. Bond and Daniel F. Litim
Department of Physics and Astronomy, University of Sussex, Brighton BN1 9QH, United Kingdom

(Received 24 February 2022; accepted 13 April 2022; published 11 May 2022)

We demonstrate that interacting ultraviolet fixed points in four dimensions exist at strong coupling and away from large-N Veneziano limits. This is established exemplarily for semisimple supersymmetric gauge theories with chiral matter and superpotential interactions by using the renormalization group and exact methods from supersymmetry. We determine the entire superconformal window of ultraviolet fixed points as a function of field multiplicities. Results are in accord with the a-theorem, bounds on conformal charges, Seiberg duality, and unitary. We also find manifolds of Leigh-Strassler models exhibiting lines of infrared fixed points. At weak coupling, findings are confirmed using perturbation theory up to three loop. Benchmark models with low field multiplicities are provided, including examples with Standard-Model-like gauge sectors. Implications for particle physics, model building, and conformal field theory are indicated.

DOI: 10.1103/PhysRevD.105.105005

I. INTRODUCTION

Ultraviolet fixed points are key for the renormalizability and predictive power of quantum field theories. The classic example is given by asymptotic freedom of the strong nuclear force, where the fixed point is noninteracting [1,2]. The possibility of interacting ultraviolet (UV) fixed points, often denoted as asymptotic safety [3], has been conjectured early on [4]. Recently, this field has taken up some speed due to the discovery of UV conformal fixed points in models of particle physics [5–10]. Conditions under which asymptotic safety arises in weakly coupled four-dimensional quantum field theories (without gravity) are by now well understood: Non-Abelian gauge fields are central [6], alongside Yukawa and scalar interactions and subject to a stable vacuum [7,8]. Templates with strict perturbative control have been found for unitary [5], orthogonal and symplectic [9], or product gauge groups [10], and supersymmetry [11]. This has also triggered new ideas for model building [12,13], asymptotically safe extensions of the Standard Model explaining the electron and muon $g-2$ anomalies [14–16] whose new type of flavor phenomenology can be tested at colliders [17], and explanations of flavor anomalies as evidenced in rare B-meson decays [18]. Further results cover vacuum stability [19] including the Higgs [14–16,18], Abelian factors [13], global fixed points [20], aspects of radiative symmetry breaking [21], UV conformal windows [22], and fixed point mergers [23].

Published by the American Physical Society under the terms of the Creative Commons Attribution 4.0 International license. Further distribution of this work must maintain attribution to the author(s) and the published article's title, journal citation, and DOI. Funded by SCOAP³.

Despite the vast body of weakly coupled fixed points at hand, it has remained an open challenge to understand asymptotic safety of strongly coupled 4D quantum field theories from first principles. It would be desirable to have rigorous and explicit examples at hand, if only as a proof of principle, and to clarify whether large matter field anomalous dimensions or new phenomena may become an obstacle for safety in the UV. Moreover, it is well known that weakly coupled fixed points often require a large number of gauge and matter fields, such as in a Veneziano large-N limit, while decreasing the number of matter fields turns fixed point interactions stronger. In the context of asymptotically safe model building where only finitely many new matter fields are added to the Standard Model [12–18], it becomes paramount to control the size of UV conformal windows nonperturbatively and to understand how few matter fields can sustain an underlying fixed point [22,23]. It would be equally important to understand whether or not qualitatively new types of fixed points arise at strong coupling, beyond those discovered at weak coupling.

In this spirit, we put forward a nonperturbative search for interacting UV fixed points in conventional 4D quantum field theories, without gravity. With asymptotically safe fixed points being presently out of reach for lattice simulations or the conformal bootstrap, we turn, instead, to $N=1$ global supersymmetry as the nonperturbative tool of choice: Nonrenormalization theorems ensure that superpotential (Yukawa) couplings are renormalized nonperturbatively via the chiral superfield anomalous dimensions, and exact infinite-order perturbative renormalization group (RG) equations are available for gauge couplings [24,25]. Further, at superconformal fixed points, anomalous dimensions of all chiral superfields can be determined unambiguously using the method of a-maximization [26]. Finally, independent

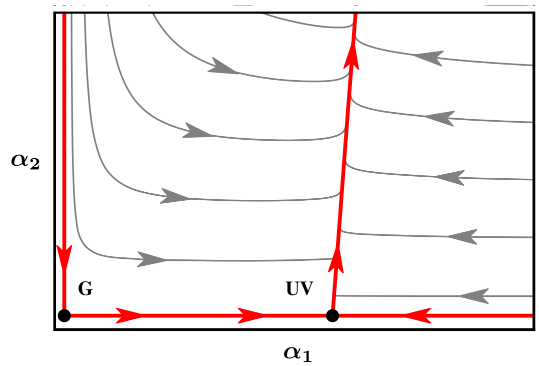

FIG. 1. The basic setup in the plane of gauge couplings (α_1, α_2), showing the free Gaussian fixed point (G) and an interacting ultraviolet fixed point (UV), with arrows on RG trajectories pointing from the UV to the IR. Note that the Gaussian is a "saddle" and asymptotic freedom is absent.

quartics do not arise and vacuum stability is automatically guaranteed provided gauge and Yukawa couplings take viable fixed points. Taken together, these ingredients prove sufficient to determine interacting fixed points reliably, including at strong coupling.

Here, we apply this methodology exemplarily to an asymptotically nonfree $SU(N_1) \times SU(N_2)$ supersymmetric gauge theory, with massless chiral matter and a superpotential, and determine the entire conformal window of interacting UV fixed points. Our basic setup is illustrated in Fig. 1 which shows the phase diagram of a semisimple gauge theory with superpotential interactions. Notice that asymptotic freedom is absent because one of the gauge sectors (α_2) is infrared-free while the other is not (α_1). The theory may nevertheless develop an asymptotically safe fixed point (UV) which allows a well-defined high energy limit and outgoing RG trajectories toward the IR and which is the central topic of this study. Consistency with Seiberg duality, and constraints from the a-theorem, global charges, and unitarity, are also observed [27]. Findings are confirmed independently using perturbation theory up to three-loop order. Implications of our findings for the asymptotic safety conjecture, model building, and conformal field theory are indicated.

II. SEMISIMPLE GAUGE THEORIES WITH MATTER

We consider semisimple Yang-Mills theories with product gauge group $SU(N_1) \times SU(N_2)$ coupled to chiral superfields (ψ, χ, Ψ, Q) with flavor multiplicities $(N_F, N_F, 1, N_Q)$ and gauge charges as in Table I. We require that the model has a global $N = 1$ supersymmetry. It is then characterized by two gauge couplings g_1 and g_2 and a Yukawa coupling y via the superpotential

$$W = y\mathrm{Tr}[\psi_L \Psi_L \chi_L + \psi_R \Psi_R \chi_R], \tag{1}$$

TABLE I. Chiral matter with gauge charges and multiplicities.

Matter	ψ_L	ψ_R	Ψ_L	Ψ_R	χ_L	χ_R	Q_L	Q_R
$SU(N_1)$	$\bar{\square}$	$\square$	$\square$	$\bar{\square}$	1	1	1	1
$SU(N_2)$	1	1	$\square$	$\bar{\square}$	$\bar{\square}$	$\square$	$\bar{\square}$	$\square$
Flavor	N_F	N_F	1	1	N_F	N_F	N_Q	N_Q

where the trace sums over flavor and gauge indices. The superfields Q are not furnished with Yukawa interactions. The theory has a global $SU(N_F)_L \times SU(N_F)_R \times SU(N_Q)_L \times SU(N_Q)_R$ flavor and a $U(1)_R$ symmetry and is characterized by the field multiplicities

$$(N_1, N_2, N_F, N_Q). \tag{2}$$

Asymptotic freedom and interacting infrared fixed points arise for suitable matter field multiplicities. For this study, the regime of interest is where the $SU(N_1)$ gauge sector is asymptotically free while the $SU(N_2)$ gauge sector is infrared-free. Accordingly, the free theory corresponds to a saddle and asymptotic freedom cannot be achieved (Fig. 1), very much like in the non-Abelian gauge sectors of the minimal supersymmetric standard model (MSSM). In this light, the gauge coupling α_2 can be viewed as "dangerously irrelevant," in that it may become relevant due to the gauge-Yukawa fixed point in the other gauge sector.

In the large-N Veneziano limit, the theory has previously been studied in perturbation theory, where it was found that interacting UV fixed points can arise at weak coupling with perturbatively small anomalous dimensions [11]. The main point of this study is to investigate the conditions under which theories with (6) may develop strongly interacting ultraviolet fixed points where anomalous dimensions become large, of order unity. Ordinarily, this would require strong coupling methods such as lattice simulations to establish the claim. In supersymmetry, however, powerful continuum methods beyond perturbation theory are available, to which we turn next.

III. RENORMALIZATION GROUP

To achieve our claim, we must find the renormalization group equations for all couplings and identify their fixed points and nonperturbative expressions for the chiral superfield anomalous dimensions. Here, we exploit key features of $N = 1$ supersymmetric gauge theories that make this task feasible.

For supersymmetric gauge theories, closed all-order expressions for perturbative β-functions have been achieved by Novikov *et al.* (NSVZ) [24,25] (see also [28,29]). We introduce the gauge and Yukawa couplings as

$$\alpha_{1,2} = \left(\frac{g_{1,2}}{4\pi}\right)^2, \qquad \alpha_y = \left(\frac{y}{4\pi}\right)^2 \tag{3}$$

and denote the chiral superfield anomalous dimensions as γ_a $(a = \psi, \Psi, \chi, Q)$, with β-functions $\beta_i \equiv d\alpha_i/d\ln\mu (i = 1, 2, y)$ defined as usual. The NSVZ beta functions for the gauge couplings of our models are then given by

$$\beta_1 = \frac{2\alpha_1^2}{F(\alpha_1)}[N_F(1-2\gamma_\psi) + N_2(1-2\gamma_\Psi) - 3N_1], \tag{4}$$

$$\beta_2 = \frac{2\alpha_2^2}{F(\alpha_2)}[N_F(1-2\gamma_\chi) + N_1(1-2\gamma_\Psi) + N_Q(1-2\gamma_Q) - 3N_2]. \tag{5}$$

The scheme-dependent function $F(\alpha)$ is normalized to unity for vanishing coupling [30] and reads $F(\alpha) = 1\text{–}2C_2^G\alpha$ in the NSVZ scheme [24,25] with C_2^G the quadratic Casimir in the adjoint. Close to the Gaussian fixed point, the anomalous dimensions vanish and we can then read off the condition for a saddle in terms of the field multiplicities (2),

$$\begin{aligned} 3N_1 &> N_2 + N_F, \\ 3N_2 &\le N_1 + N_F + N_Q. \end{aligned} \tag{6}$$

This also covers the case where the one-loop coefficient of β_2 vanishes identically. For the Yukawa coupling, we exploit that supersymmetry dictates strict nonrenormalization theorems, which ensure that superpotential couplings are only renormalized through field anomalous dimensions. Hence, the RG running is given by

$$\beta_y = 2\alpha_y[\gamma_\psi + \gamma_\Psi + \gamma_\chi], \tag{7}$$

valid to all orders in perturbation theory. Renormalization group fixed points $(\beta_i = 0)$ correspond to superconformal field theories.

All perturbative fixed points $(\alpha_i^* \ll 1)$ for this theory have previously been found in [11]. In general, these are either Banks-Zaks fixed points, where some of the gauge couplings are nonzero but $\alpha_y^* = 0$, or gauge-Yukawa (GY) fixed points with one (GY_1), the other (GY_2), or both gauge couplings nonzero (GY_{12}) and $\alpha_y^* > 0$ [6,7]. It has also been shown that if GY_1 is UV, its outgoing trajectory is connected with the IR fixed point (GY_{12}), and similarly for GY_2 [11].

In this work, we focus on the regime (6) and search for nonperturbative fixed points with the property

$$\mathrm{GY}_1:\ \alpha_1^* > 0, \qquad \alpha_y^* > 0, \qquad \alpha_2^* = 0. \tag{8}$$

Our ansatz states that the $SU(N_2)$ gauge sector is infrared-free, meaning $\beta_2 > 0$ in the vicinity of the Gaussian. If $\beta_2 < 0$ in the vicinity of the interacting fixed point, the $SU(N_2)$ gauge sector suddenly becomes asymptotically free, and the fixed point is ultraviolet. In its vicinity, α_2 is the only relevant coupling in the UV, which runs out of the fixed point as

$$\alpha_2(\mu) = \frac{\delta\alpha_2(\Lambda)}{1 + B_{2,\mathrm{eff}}\delta\alpha_2\ln(\mu/\Lambda)}, \tag{9}$$

with $\delta\alpha_2(\Lambda)$ a small deviation at the high scale Λ, $B_{2,\mathrm{eff}} = B_2 + N_F\gamma_\chi + 4N_1\gamma_\Psi > 0$ the interaction-induced one-loop coefficient, and $B_2 < 0$ given by (minus) the one-loop coefficient of (5) at the Gaussian. The couplings α_1 and α_y are irrelevant interactions in the UV and their running is fully determined by the one of α_2 [11]. This scenario is schematically depicted in Fig. 1.

The necessary and sufficient conditions for the partially interacting fixed point to turn the dangerously irrelevant coupling α_2 into a relevant one are given by

$$\begin{aligned} 0 &= 3N_1 - N_F(1-2\gamma_\psi) - N_2(1-2\gamma_\Psi), \\ 0 &< 3N_2 - N_F(1-2\gamma_\chi) - N_1(1-2\gamma_\Psi) - N_Q(1-2\gamma_Q), \\ 0 &= \gamma_\psi + \gamma_\Psi + \gamma_\chi, \end{aligned} \tag{10}$$

where the two equations determine the fixed point, while the inequality ensures the sign flip from $\beta_2 \ge 0$ close to the Gaussian to $\beta_2 < 0$ close to the fixed point (8).

IV. *a*-MAXIMIZATION

The beta functions (4), (5), and (7), and the conditions (10), still depend on the superfield anomalous dimensions. These can be determined either perturbatively, as we will do in Sec. VIII below, or exactly, as we do here. To that end, we exploit that fixed points of the renormalization group correspond to superconformal field theories. Hence, superfields must transform in representations of the superconformal algebra. Focusing on the bosonic part, we observe an extra global $U(1)_R$ symmetry in addition to the ordinary conformal algebra. The global and anomaly free $U(1)_R$ symmetry prescribes global charges R_i for all chiral superfields at any superconformal fixed point and thereby determines anomalous dimensions γ_i of chiral superfields via

$$\gamma_i = \frac{3}{2}R_i - 1. \tag{11}$$

The task then reduces to the determination of R-charges at superconformal fixed points for which we use the method of a-maximization [26]. Specifically, at the fixed point GY_1 with (8) and characterized by (10), we find

$$
\begin{aligned}
R_\psi &= \frac{2}{3}(1+\gamma_\psi) = \frac{N_F[N_F-(N_1+N_2)]^2 - N_1^2 N_2 \Delta}{[N_2-N_F][N_1(N_2+N_F)+(N_2-N_F)^2]},\\
R_\Psi &= \frac{2}{3}(1+\gamma_\Psi) = \frac{N_2[N_2-(N_1+N_F)]^2 - N_1^2 N_F \Delta}{[N_F-N_2][N_1(N_2+N_F)+(N_2-N_F)^2]},\\
R_\chi &= \frac{2}{3}(1+\gamma_\chi) = \frac{8}{9}\frac{(N_2-N_F)^2}{(N_2-N_F)^2-(1-\Delta)N_1^2},\\
R_Q &= \frac{2}{3}(1+\gamma_Q) = \frac{2}{3}, \qquad (12)
\end{aligned}
$$

and $\Delta > 0$ the positive root of

$$
\Delta^2 = 1 + \left(\frac{N_2-N_F}{3N_1^2}\right)^2 [(4N_1+N_2+N_F)^2 - 34N_1^2 - 4N_2N_F]. \qquad (13)
$$

The ψ_Q fermions do not interact at the fixed point (8), hence $\gamma_Q = 0$ and none of the R-charges depend on N_Q. The results for the R-charges uniquely determine the remaining anomalous dimensions nonperturbatively and provide closure for the beta functions (4), (5), and (7). At weak coupling, anomalous dimensions are small and R-charges are close to their classical values ($R_i \approx \frac{2}{3}$). Moreover, unitarity mandates that scaling dimensions D of spinless operators must satisfy $D \geq 1$ [27], additionally implying $\gamma_i \geq -\frac{1}{2}$ ($R_i \geq \frac{1}{3}$) for gauge-invariant scalar operators such as $\bar\psi\psi$.

The conditions for unitary quantum field theories with interacting UV fixed points (10) only depend on ratios of field multiplicities. Therefore, we can reduce the four-dimensional parameter space of field multiplicities (2) to a three-dimensional one. Following [11], we do so by scaling-out one of the field multiplicities, say N_1, and by introducing three suitable ratios of field multiplicities instead,

$$
R = \frac{N_2}{N_1}, \quad P = \frac{N_1}{N_2}\frac{N_Q+N_1+N_F-3N_2}{N_F+N_2-3N_1}, \quad \epsilon = \frac{N_F+N_2}{N_1} - 3. \qquad (14)
$$

The color ratio R (not to be confused with the R-charges R_i) is sensitive to the relative size of gauge groups. The parameter $P < 0$ is proportional to the ratio of one-loop gauge coefficients. The parameter ϵ, which in the region of interest is negative $\epsilon < 0$, can be made arbitrarily small in a Veneziano limit where it controls perturbative fixed points provided $|\epsilon| \ll 1$. Since field multiplicities are semipositive numbers, we further observe

$$
0 < R < 3, \quad P < \frac{4(1-R)+\epsilon}{R\epsilon}, \quad R-3 < \epsilon < 0. \qquad (15)
$$

The parameters (14) take discrete values for integer field multiplicities except in a Veneziano large-N limit where they become continuous.

V. FIXED POINTS AND CONFORMAL WINDOWS

We are now in a position to investigate the range of field multiplicities for which the theory displays an interacting ultraviolet fixed point. Exploiting all constraints, we find that the parameter P is bounded from above and from below

$$
P_{\min}(R,\epsilon) < P \leq P_{\max}(R,\epsilon). \qquad (16)
$$

The upper boundary $P_{\max}$ relates to (6) and $P \leq 0$, and to the physicality of field multiplicities (15), whichever is stronger. The lower boundary $P_{\min}$ relates to the sign flip for induced asymptotic freedom of $SU(N_2)$. Explicitly,

$$
P_{\max}(R,\epsilon) = \begin{cases} \frac{4(1-R)+\epsilon}{R\epsilon} & \text{for } R < 1+\frac{\epsilon}{4}, \\ 0 & \text{otherwise} \end{cases} \qquad (17)
$$

$$
P_{\min}(R,\epsilon) = \frac{3R_\Psi - 2}{R\epsilon} + \frac{(3R_\chi-2)(3-R+\epsilon)}{R\epsilon}. \qquad (18)
$$

In the above, the R-charges R_Ψ and R_χ are understood as functions of (R,ϵ) via (12) and (14). The parameters R and ϵ are constrained globally by the physicality of couplings ($\alpha \geq 0$) and unitarity,

$$
\frac{1}{4} < R < 2 \quad \text{and} \quad -\frac{3}{2} \leq \epsilon < 0. \qquad (19)
$$

Figure 2 shows a contour plot of the superconformal window (16) and (19) in the (ϵ, R) plane. The left panel shows the lower boundary $P_{\min}$, while the right panel shows the accessible range of P values between $P_{\min}$ and $P_{\max}$. The lower boundary in both graphs is given by $R_{\min} = 1+\frac{\epsilon}{2}$, corresponding to $N_1 + N_2 = N_F$. Above the full white line $R = 1+\frac{\epsilon}{4}$, we have $P_{\max} = 0$. Roughly speaking, the width in P is largest around the full white line. The upper boundary $R_{\max}(\epsilon)$ arises as the solution of a cubic, approximately given by $R_{\max} \approx 2 + \frac{2}{3}\epsilon$ where $N_2 = N_F$. We notice that the width $P_{\max} - P_{\min}$ vanishes at $R_{\max}$, while it remains small but non-zero at $R_{\min}$, except at the end points. Weakly coupled fixed points correspond to parameters (P, R, ϵ) close to the boundary where $|\epsilon| \ll 1$.

The conformal window is further illustrated in Fig. 3 showing its projection onto the (P, R) plane. Within the yellow-shaded area, weakly coupled fixed points arise toward the right of the dashed line, while strongly coupled fixed points can arise anywhere. Outside the yellow-shaded area, asymptotic safety is not available and the corresponding quantum field theories must be viewed as effective rather than fundamental.

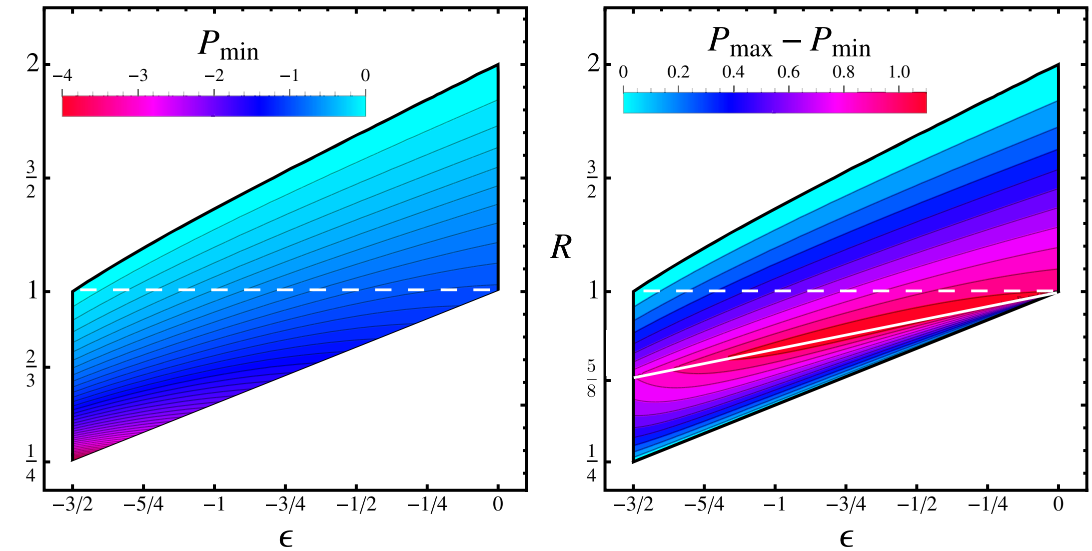

FIG. 2. Contour plot of the superconformal window for asymptotic safety (16) in the (R, ϵ) plane showing the boundary $P_{\rm min}$ (left) and the height $P_{\rm max} - P_{\rm min}$ (right); dashed and full white lines are explained in the main text.

It is interesting to discuss the N_F dependence of fixed points within the conformal window while keeping (N_1, N_2, P) fixed. In Fig. 2, this effectively corresponds to varying ϵ along horizontal cuts. We notice that the conformal window splits into two distinct types of models, separated by dashed lines in Figs. 2 and 3, to which we refer as "mostly weakly" and "mostly strongly" coupled. Specifically, the first subset of models are those above the dashed line in Fig. 2 and on the right of the dashed line in Fig. 3. Their conformal window is characterized by

$$1 \le R < 2. \tag{20}$$

Then, for any admissible value of R within (20), there is a range of viable parameters P within $(-1, 0]$ such that the UV conformal window in ϵ covers the range

$$\epsilon_{\rm max} \le \epsilon < 0. \tag{21}$$

The lower bound $\epsilon_{\rm max} = \frac{3}{2}(R-2)$ may become as low as $-\frac{3}{2}$. The significance of this result is as follows. Perturbative fixed points are controlled by the parameter $|\epsilon| \ll 1$ in a large-N Veneziano limit, meaning that this part of the UV conformal window contains all perturbatively controlled superconformal UV fixed points found previously in [11]. Hence, we observe that all perturbative fixed points extend into a nonperturbative conformal window for ϵ given precisely by the range (21). The same considerations apply for finite N, away from a Veneziano limit, the only difference being that (R, P, ϵ) take discrete rather than continuous values. Since all theses fixed points are linked to weakly coupled ones, and for want of terminology, we refer to the models within (20) as mostly weakly coupled.

Next, we turn to the part of the conformal window below the dashed line in Fig. 2 and to the left of the dashed line in Fig. 3, characterized by

$$\frac{1}{4} < R < 1. \tag{22}$$

For any admissible value of R within (22), there is a range of viable parameters P within $(-4, 0]$ such that the UV conformal window in ϵ covers the range

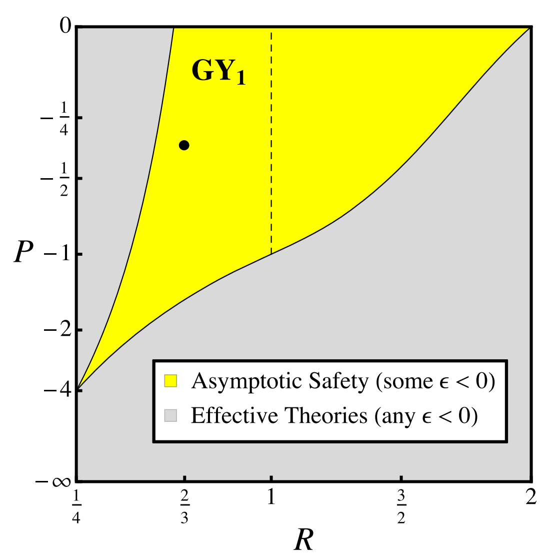

FIG. 3. Projection of the superconformal window with interacting ultraviolet fixed points onto the (R, P) parameter plane. Weakly coupled fixed points arise within the yellow-shaded area on the right of the dashed line. Strongly coupled fixed points arise within the entire yellow-shaded area for some range of ϵ. The full dot is discussed in the main text.

$$-\frac{3}{2} \leq \epsilon < \epsilon_{\min} < 0. \tag{23}$$

Here, the lower bound $\epsilon_{\min} = 2(R-1) < 0$ ensures induced asymptotic freedom for the coupling α_2. Most importantly, we observe the existence of a finite gap $[\epsilon_{\min}, 0]$ in ϵ within which no asymptotically safe fixed points can be found. This implies that none of the fixed points within (22) can be achieved with strict perturbative control ($\epsilon \to 0^-$), not even in a Veneziano limit. It is in this sense that the fixed points within (22) are nonperturbative and parametrically disconnected from the free theory, quite different from those in (20). For these reasons, we refer to these superconformal fixed points as mostly strongly coupled.

Another important aspect of the conformal window relates to the saddle close to the Gaussian which needs to be overcome by the interacting fixed point. Recall that the asymptotically free (infrared-free) direction is characterized by the one-loop gauge coefficient $B_1 = 2N_1\epsilon < 0$ ($B_2 = 2N_2P\epsilon \geq 0$), with (minus) their ratio given by the imbalance parameter

$$I = -B_2/B_1 \equiv |P| \cdot R \tag{24}$$

for which we have $I \geq 0$. Quantum effects at the interacting fixed point overcome the positive or vanishing one-loop coefficient B_2 and turn it, effectively, into a negative one (see Fig. 1). It is then important to understand the largest imbalance that can be achieved without spoiling asymptotic safety. We find that the imbalance is bounded from above,

$$0 \leq I = \frac{3N_2 - N_1 - N_F - N_Q}{N_F + N_2 - 3N_1} < 1, \tag{25}$$

where we recall that field multiplicities obey (6). In other words, as soon as one gauge sector is as or more infrared-free at the Gaussian fixed point than the other gauge sector is ultraviolet-free, asymptotic safety at an interacting fixed point cannot arise.

In Figs. 2 and 3, the small imbalance region $0 \leq I \ll 1$ is realized close to the upper boundaries where $P \approx 0$. Here, many ultraviolet fixed points can be found in large parts of the parameter space including perturbative and nonperturbative ones. With growing imbalance $I \to 1$, the set of perturbatively controlled fixed points shrinks to the vicinity of a single point $(P, R) = (-1, 1)$.[1] Nonperturbatively, however, many more fixed points realize a near-maximal imbalance, corresponding to the lower boundary in Fig. 2 with parameters given by the line $R = R_{\min}(\epsilon)$, $P = -1/R_{\min}$, and $\epsilon \in [-\frac{3}{2}, 0)$. In Fig. 3, the near-maximal imbalance is realized along the lower boundary to the left of the dashed line. We conclude that all models that may afford the near-maximal imbalance are contained in the mostly strongly coupled part of the conformal window (22).

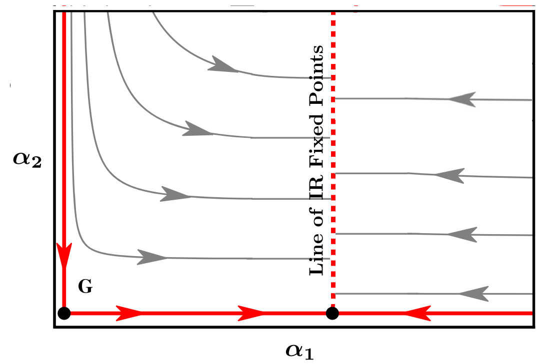

FIG. 4. Schematic phase diagram of Leigh-Strassler-type models in the plane of gauge couplings in the limit where the UV fixed point degenerates into a line of IR fixed points (see Fig. 1).

We emphasize that the boundary at $P_{\min}$ in (18) is not part of the conformal window. The reason for this is that whenever $P \to P_{\min}$ the inequality in (10) becomes an equality, meaning that $\beta_2 \to 0$ nonperturbatively at the fixed point (8). At this point the UV fixed point GY_1 merges with yet another fixed point (a nonperturbative IR fixed point GY_{12} [11]) in the limit $P \to P_{\min}$. In consequence, the fixed point (8) degenerates into a line of fixed points for any α_2, illustrated in Fig. 4. As such, this limit offers a manifold of Leigh-Strassler-type models [31], each of which is characterized by a line of interacting superconformal field theories, disconnected from the free theory and generated by an exactly marginal operator. Further, each of these lines of fixed points corresponds to an infrared sink because the previously relevant perturbation, given by α_2, has become strictly marginal. This includes all settings with maximal imbalance $I = 1$. Concrete examples for strongly coupled Leigh-Strassler models are delegated to Sec. X below.[2]

Figure 5 shows the superfield anomalous dimensions within the entire conformal window. Since the spectator fermions ψ_Q are free at the fixed point (8), the chiral superfield anomalous dimensions are only functions of (R, ϵ) and independent of P. Overall, we find that anomalous dimensions grow with growing $|\epsilon|$. For models within (20) or (22), the chiral anomalous dimensions cover the range

$$0 > \gamma_\psi, \gamma_\Psi \geq -\frac{1}{2} \quad \text{and} \quad 0 < \gamma_\chi \leq 1 \tag{26}$$

[1] In a Veneziano limit, this are the models with $N_1, N_2, N_F \to \infty$, while $N_F/N_1 = N_F/N_2 = 2$ and $N_Q/N_1 \to 0$.

[2] The fate of an IR sink can be evaded by adding mass term perturbations for the N_F superfields ψ, which may lift the degeneracy and allow RG trajectories to emanate from the line of fixed points. However, this mechanism defies the original setup (6) in that the removal of the ψ degrees of freedom would make the theory asymptotically free from the outset.

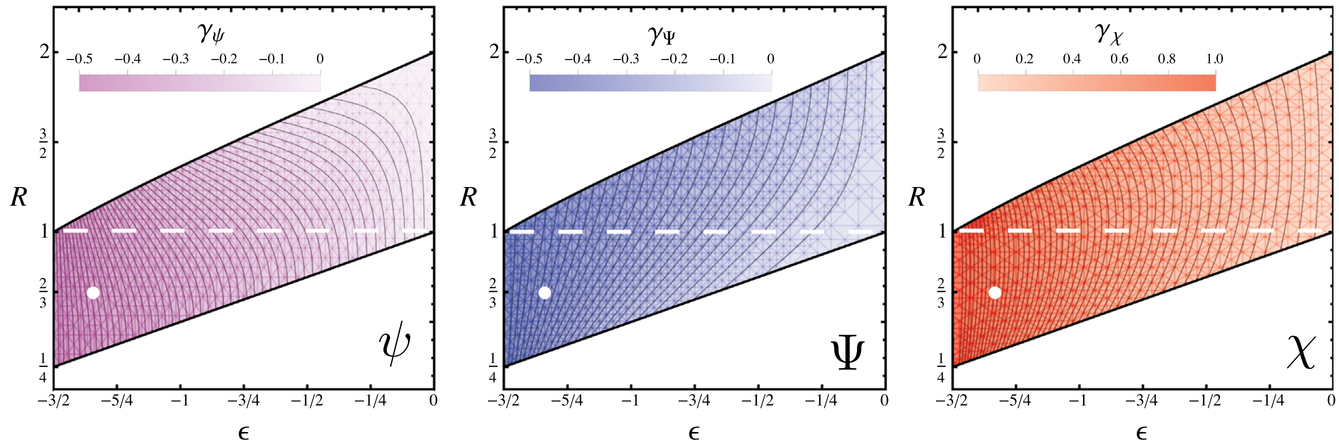

FIG. 5. Contour plot showing the nonperturbative anomalous dimensions of chiral superfields at the superconformal fixed points of Fig. 2. The full dot and dashed line are explained in the main text.

with extremals reached at the $\epsilon = -\frac{3}{2}$ and $\epsilon = 0$ boundaries of the conformal window. For models within (22) anomalous dimensions tend to take larger values than for those in (20). A comparison with perturbation theory is given in Sec. VIII. Incidentally, the monotonicity of γ_i with growing ϵ establishes that anomalous dimensions do not vanish unless the fixed point is free.

VI. CENTRAL CHARGES AND THE *a*-THEOREM

Superconformal fixed points can also be characterized by central charges a, b, and c, the anomaly coefficients [32,33]. Their values have to satisfy certain conditions and can be used to constrain viable fixed points. The global charges a and c can be expressed in terms of the R-charges of chiral superfields,

$$a = \frac{3}{32}(3\mathrm{Tr}R^3 - \mathrm{Tr}R), \tag{27}$$

$$c = \frac{1}{32}(9\mathrm{Tr}R^3 - 5\mathrm{Tr}R). \tag{28}$$

Given that the positivity conditions $a, b, c > 0$ are satisfied nonmarginally for free theories, they are guaranteed to be satisfied for perturbative theories. Similarly, the conformal collider bound [34]

$$\frac{1}{2} < \frac{a}{c} < \frac{3}{2} \tag{29}$$

cannot be violated for weakly interacting theories. Here, we find that the positivity conditions and the conformal collider bound are satisfied nonperturbatively, in the entire conformal window, as they must.

We now turn to the a-theorem. It states that the central charge a must be a decreasing function along RG trajectories in any 4D quantum field theory [35,36]. We find that $a_{\mathrm{UV}} - a_{\mathrm{Gauss}} < 0$, which confirms that none of the UV fixed points is connected by an RG trajectory with the free Gaussian fixed point, in accord with Fig. 1. Further, we noted earlier that any interacting UV fixed point in the conformal window comes bundled with a fully interacting nonperturbative IR fixed point (GY_{12}) [11]. We find $a_{\mathrm{UV}} - a_{\mathrm{IR}} > 0$, meaning that both conformal fixed points are connected by RG trajectories flowing from the former to the latter as in Fig. 1. We conclude that our results are consistent with the a-theorem, as they must.

VII. SEIBERG DUALITY

Next, we comment on how our results relate to Seiberg's electric-magnetic duality [37]. At the partially interacting fixed point (8) where the $SU(N_2)$ gauge sector is free, the flavor symmetry of the theory is enhanced. This manifests itself as an exchange symmetry under $N_2 \leftrightarrow N_F$, whereby the quarks ψ and Ψ interchange their roles while the fields χ remain unchanged,

$$N_2 \leftrightarrow N_F, \qquad R_\psi \leftrightarrow R_\Psi, \qquad R_\chi \leftrightarrow R_\chi, \tag{30}$$

see (12). Hence, we observe an interacting "magnetic" $SU(N_1)$ gauge theory which has $N_F + N_2$ flavors of "magnetic quarks" ψ and Ψ, alongside $(N_F + N_2)^2$ singlet mesons $(\psi_L \psi_R)$, χ_L, χ_R, and $(\Psi_L \Psi_R)$ [38]. In this light, the gauge-Yukawa fixed point (8) corresponds to a free non-Abelian magnetic phase whose superconformal window is known to cover the range $\frac{3}{2}N_1 < N_F + N_2 < 3N_1$ [37], which corresponds to the parameter range $-\frac{3}{2} < \epsilon < 0$ observed in (19). Notice, however, that the conformal window in Fig. 2 has additional constraints on (R, P) that ensure that the $SU(N_2)$ gauge sector becomes a relevant perturbation at the fixed point.

Seiberg duality predicts the existence of a dual "electric" theory which must have gauge group $SU(N_F + N_2 - N_1)$ coupled to $N_F + N_2$ flavors of electric quarks. The conformal window of the non-Abelian Coulomb phase is given by $\frac{3}{2}(N_F+N_2-N_1)<N_F+N_2<3(N_F+N_2-N_1)$. This corresponds to the exact same parameter band in ϵ as the one in (19). In the special case where $N_F=N_2$, given by the upper boundary in Fig. 2, the R-charges simplify and become

$$R_\psi = R_\Psi = 1-\frac{N_1}{2N_F}, \qquad R_\chi = \frac{N_1}{N_F}. \tag{31}$$

One recognizes the R-charges for the quarks and singlet mesons of supersymmetric magnetic QCD [37], whose Seiberg dual is characterized by electric quarks $\tilde\psi$ and $\tilde\Psi$ with

$$R_{\tilde\psi} = R_{\tilde\Psi} = \frac{N_1}{2N_F}. \tag{32}$$

We refer to [38] for further aspects of Seiberg duality in theories with product gauge groups.

VIII. PERTURBATION THEORY

In this section, we contrast the nonperturbative determination of anomalous dimensions with perturbation theory, using general expressions for perturbative beta functions up to three loop, obtained in the dimensional reduction scheme [39,40]. The main additions are perturbative expressions for anomalous dimensions which at superconformal fixed points can be used to cross-check the nonperturbative results from a-maximization.

For the sake of this comparison, it is convenient to perform a Veneziano limit and rescale gauge couplings as $\alpha_i \to N_i\alpha_i$ and Yukawa couplings as $\alpha_y \to N_1\alpha_y$. We also use the parametrization (14). The parameter $0<|\epsilon|\ll 1$ then serves as a small expansion parameter to ensure rigorous control of fixed points in perturbation theory. To find fixed points, scaling exponents, and anomalous dimensions to first (second) order in ϵ, we must retain terms up to two (three) loop in the gauge coupling and up to one (two) loop in the Yukawa beta functions [7,22]. We refer to these approximations as next-to-leading order (NLO) and next-to-next-to-leading order (NNLO), respectively. Using the general results of [39,40] we find the gauge beta functions up to three loop for our models as

$$\begin{aligned}
\beta_1^{(1)} &= 2\alpha_1^2\epsilon,\\
\beta_1^{(2)} &= 2\alpha_1^2[6\alpha_1+2R\alpha_2-4R(3+\epsilon-R)\alpha_y],\\
\beta_1^{(3)} &= 4\alpha_1^2[2\epsilon\alpha_1^2-R(2\alpha_1\gamma_\Psi^{(1)}+\gamma_\Psi^{(2)})\\
&\quad -(3+\epsilon-R)(2\alpha_1\gamma_\psi^{(1)}+\gamma_\psi^{(2)})],
\end{aligned} \tag{33}$$

and

$$\begin{aligned}
\beta_2^{(1)} &= 2\alpha_2^2P\epsilon,\\
\beta_2^{(2)} &= 2\alpha_2^2\left[6\alpha_2+\frac{2}{R}\alpha_1-\frac{4}{R}(3-R+\epsilon)\alpha_y\right],\\
\beta_2^{(3)} &= 4\alpha_2^2\left[2P\epsilon\alpha_2^2-\frac{1}{R}(2\alpha_2\gamma_\Psi^{(1)}+\gamma_\Psi^{(2)})\right.\\
&\quad -\frac{3-R+\epsilon}{R}(2\alpha_2\gamma_\chi^{(1)}+\gamma_\chi^{(2)})\\
&\quad \left.-\left(4+P\epsilon-\frac{4+\epsilon}{R}\right)(2\alpha_2\gamma_Q^{(1)}+\gamma_Q^{(2)})\right].
\end{aligned} \tag{34}$$

The perturbative Yukawa beta function is given by (7) for any loop order. The anomalous dimensions of the superfields are required up to two-loop accuracy. They read

$$\begin{aligned}
\gamma_\psi^{(1)} &= R\alpha_y-\alpha_1,\\
\gamma_\Psi^{(1)} &= (3-R+\epsilon)\alpha_y-\alpha_1-\alpha_2,\\
\gamma_\chi^{(1)} &= \alpha_y-\alpha_2,\\
\gamma_Q^{(1)} &= -\alpha_2,
\end{aligned} \tag{35}$$

and

$$\begin{aligned}
\gamma_\psi^{(2)} &= -R\alpha_y(\gamma_\Psi^{(1)}+\gamma_\chi^{(1)})-\alpha_1\gamma_\psi^{(1)}+4\epsilon\alpha_1^2,\\
\gamma_\Psi^{(2)} &= -(3-R+\epsilon)\alpha_y(\gamma_\psi^{(1)}+\gamma_\chi^{(1)})-(\alpha_1+\alpha_2)\gamma_\Psi^{(1)}\\
&\quad +4\epsilon\alpha_1^2+4P\epsilon\alpha_2^2,\\
\gamma_\chi^{(2)} &= -\alpha_y(\gamma_\psi^{(1)}+\gamma_\Psi^{(1)})-\alpha_2\gamma_\chi^{(1)}+4P\epsilon\alpha_2^2,\\
\gamma_Q^{(2)} &= -\alpha_2\gamma_Q^{(1)}+4P\epsilon\alpha_2^2,
\end{aligned} \tag{36}$$

respectively. Then, interacting fixed points with (8) are determined via a Taylor expansion of couplings in ϵ around the zeros of (33) and (7), also using (35) and (36). Notice that (34) is only used to determine whether the sign change from $\beta_2>0$ at the Gaussian to $\beta_2<0$ at (8) has taken place. Inserting the perturbative results for the fixed point into (35) and (36) provides explicit expressions for the anomalous dimensions of the form

$$\gamma_i(\epsilon) = A_i^{(1)}\epsilon + A_i^{(2)}\epsilon^2 + \mathcal{O}(\epsilon^3). \tag{37}$$

The six coefficients $A_i^{(n)}$ for $i=\psi,\Psi,\chi$ which for $n=1,2$ arise from the perturbative fixed point solutions at NLO and NNLO accuracy [10,22] still depend on the parameter R (but not on P). Their explicit expressions are not given because they do not offer further insights for the present purposes.

The expressions (37) must be compared with the exact R-charges from a-maximization (12). Writing the exact anomalous dimensions in terms of the R-charges, and expanding the expressions to second order in ϵ with the

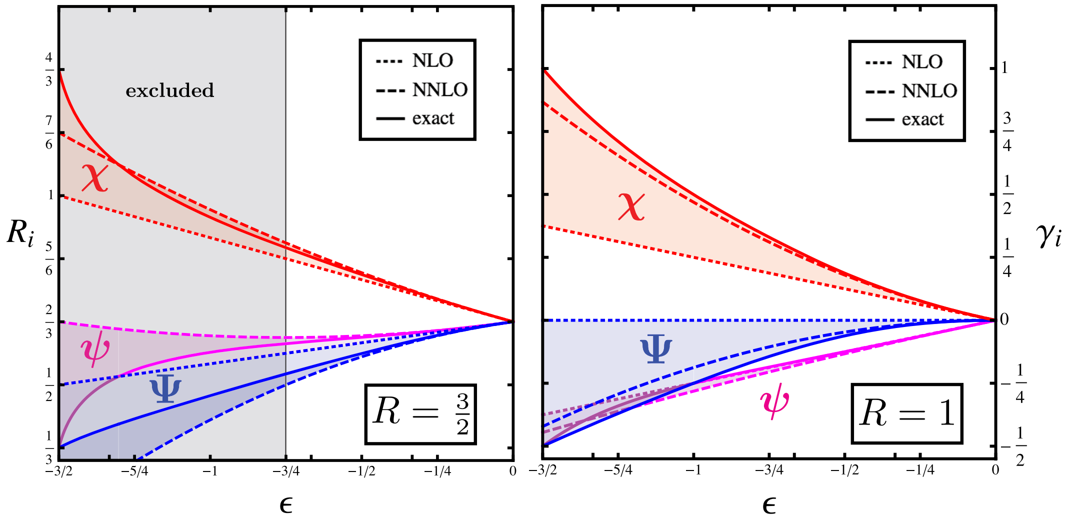

FIG. 6. Exact anomalous dimensions and $U(1)_R$ charges in comparison with two-loop (NLO) and three-loop (NNLO) results from perturbation theory. Shown are projections along $R = \frac{3}{2}$ (left) and $R = 1$ (right). Fixed points in the gray-shaded area do not show the required sign flip in (10) for any P and are therefore outside of the UV conformal window.

help of (14), we find the identical result for the coefficients $A_i^{(n)}$ in (37). This establishes consistency of findings between a-maximization and perturbation theory, as it must.

IX. ANOMALOUS DIMENSIONS

In Fig. 5 we have shown the exact anomalous dimensions across the entire UV conformal window. Here, we have a closer look into anomalous dimensions and compare with the NLO and NNLO predictions from perturbation theory. More specifically, in Figs. 6 and 7, we compare results at fixed color ratio $R = \frac{3}{2}$, 1, $\frac{2}{3}$, and $\frac{1}{3}$, and for any ϵ within $[-\frac{3}{2}, 0]$, which corresponds to horizontal cuts across Figs. 2 and 5.

We begin with Fig. 6 where our results for $R = \frac{3}{2}$ (left panel) and $R = 1$ (right panel) are shown. For small $|\epsilon| \ll 1$, perturbation theory matches the exact results as it must. With growing $|\epsilon|$, all anomalous dimensions grow in magnitude. For $R = \frac{3}{2}$, the gray-shaded area indicates that fixed points are no longer in the UV conformal window, leading to a lower bound for ϵ, see (21). Also, the NLO results for γ_ψ and γ_Ψ coincide accidentally. At NNLO, perturbative results for all three anomalous dimensions are quite close to the exact results in the admissible range for ϵ. For $R = 1$, the extension of the conformal window is maximal. Here, anomalous dimensions correspond to the fixed points along the dashed lines in Figs. 2, 3, and 5, which marks the boundary between the mostly weakly and mostly strongly coupled quantum field theories, see (20) vs (22). Maximal values $\gamma_{\psi,\Psi} \to -\frac{1}{2}$ and $\gamma_\chi \to 1$ are reached for $\epsilon \to -\frac{3}{2}$. For γ_ψ, we observe that the NLO and NNLO results are close to the exact one over the entire range for ϵ. For γ_Ψ, the NLO correction vanishes accidentally. Similarly, for γ_χ, the NLO result strongly underestimates the exact value with growing $|\epsilon|$. However, at NNLO, perturbative results for all three anomalous dimensions are close to the exact findings in the entire range of ϵ. We conclude that differences between NNLO and exact results are moderate over the entire interval. Note that this does not hold true in general, but when it does, one may use this near coincidence to extract estimates for fixed points at strong coupling which otherwise are not easily accessible.

The same analysis is repeated in Fig. 7 for the parameter choices $R = \frac{2}{3}$ (left panel) and $R = \frac{1}{3}$ (right panel). These horizontal cuts through Fig. 2 project onto the more strongly coupled fixed points in (22). For either of these, the small ϵ regions are excluded (gray-shaded areas) because the corresponding fixed points are not ultraviolet. In the increasingly narrow regions of interest (23), which are $\epsilon \in [-\frac{3}{2}, -\frac{2}{3}]$ and $\epsilon \in [-\frac{3}{2}, -\frac{4}{3}]$, respectively, we observe that differences between NLO, NNLO, and exact results become rather large for γ_χ, γ_ψ, and γ_Ψ. Outside the UV conformal window, we also notice that γ_Ψ is no longer monotonous with ϵ, but instead changes sign for nonvanishing ϵ and taking values outside the range (26). Perhaps unsurprisingly, this confirms that the leading orders of perturbation theory cease to offer a good approximation for anomalous dimensions at strong coupling, once $|\epsilon|$ is large.

X. BENCHMARKS FOR MODELS OF PARTICLE PHYSICS

At weak coupling, ultraviolet fixed points are often characterized by a large number of field multiplicities [11]. At strong coupling, fixed points can arise with a much lower number of matter fields. Therefore, we

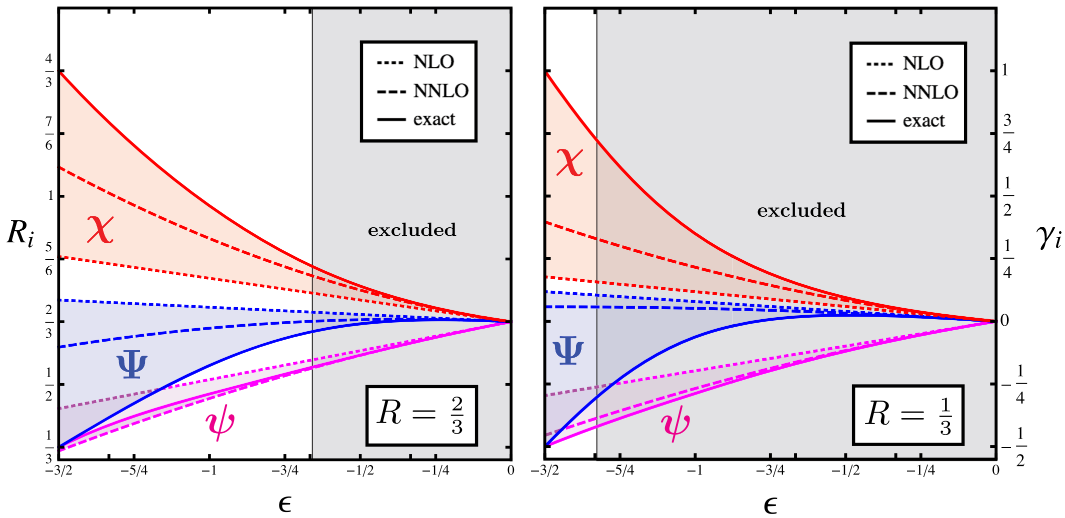

FIG. 7. Same as Fig. 6, except that the projections are along $R = \frac{2}{3}$ (left) and $R = \frac{1}{3}$ (right). Decreasing R considerably narrows the UV conformal window. The excluded (gray-shaded) areas refer to regions where some matter field field multiplicities would be unphysical (negative).

benchmark models with minimal numbers of gauge and matter fields and explore whether variants could serve as templates for asymptotically safe Standard Model extensions.

Our benchmarks of superconformal fixed points with low numbers of fields are summarized in Table II. They represent strongly coupled models in that they have large $|\epsilon|$ and anomalous dimensions. The benchmarks also cover the full range of imbalance parameters I. Note that because the ψ_Q fermions are free at the superconformal fixed point, anomalous dimensions of chiral superfields agree between different models as long as they only differ in the N_Q multiplicity, see models 2–4, models 5 and 6, or models 7 and 8.

We begin with model 1, which is the sole example with $SU(2) \times SU(2)$ gauge symmetry, the simple reason being that the only other integer solution $(N_F, N_Q) = (3, 2)$ to the constraint (6) does not lead to asymptotic safety. Here, anomalous dimensions are still small and well approximated by the perturbative three-loop result (see Fig. 6, right panel). Moreover, in models 1 and 2, the $SU(2)$ gauge sector has a vanishing one-loop coefficient. In both cases a viable interacting UV fixed point is found, located at a boundary of the conformal window (Fig. 2) where $I = 0$.

For the gauge group $SU(3) \times SU(2)$, we find a total of five solutions (models 2–6). For all of these $SU(2)$ is infrared-free at the Gaussian. Settings where $SU(3)$ is infrared-free do not lead to asymptotic safety. Also, all models are within the strongly coupled domain where three-loop perturbation theory does not offer an accurate approximation (Fig. 7, left panel). Model 3 has $N_F = 3$ and $N_Q = 1$ and its location in the conformal window is indicated by a full dot in Figs. 2 and 3. The anomalous dimensions are of order unity

$$(\gamma_\psi, \gamma_\Psi, \gamma_\chi) \approx (-0.41, -0.38, 0.79) \tag{38}$$

and shown by a full dot in Fig. 5. Enhancing N_Q by one unit gives another viable fixed point (model 4) without changing the anomalous dimensions. For $(N_F, N_Q) = (4, 0)$ (model 5) and $(N_F, N_Q) = (4, 1)$ (model 6), the main change is that $|\epsilon|$, and hence the anomalous dimensions come out slightly smaller than in models 2–4. Overall, increasing the number of matter fields charged under $SU(2)$ also increases the imbalance parameter.

Models 3–6 have some similarities with the minimal supersymmetric standard model. Unlike in the Standard Model, the $SU(2)$ sector of the MSSM becomes infrared-free due to extra gauge charges from supersymmetry partners, while the $SU(3)$ sector remains asymptotically free. Hence, the Gaussian corresponds to a saddle with imbalance $I_{\mathrm{MSSM}} = \frac{1}{3}$, just as in model 5. The imbalance could even be made larger such as in model 4 or model 6 and still yield an asymptotically safe fixed point. Hence, we see that supersymmetric gauge theories with the SM gauge groups (neglecting hypercharge) and imbalances similar to the MSSM may very well become asymptotically safe [41].

The constraints (6) imply that maximal values for anomalous dimensions (26) cannot arise if gauge group factors are as small as $SU(2)$ or $SU(3)$. For larger gauge groups, however, we can find models realizing maximal anomalous dimensions. An example is given by an $SU(6) \times SU(2)$ gauge theory with $N_F = 7$ (model 7) which has a near-maximal imbalance parameter ($I = \frac{7}{9}$). The model is located at the $\epsilon = -\frac{3}{2}$ boundary of the conformal window and leads to an asymptotically safe fixed point with nonperturbatively large chiral field anomalous dimensions,

TABLE II. Parameter and anomalous dimensions for a selection of benchmark models with superconformal fixed points and a low number of field multiplicities, including Leigh-Strassler-type models (8 and 9).

Model	Gauge group	N_F	N_Q	I	R	P	ϵ	γ_ψ	γ_Ψ	γ_χ
1	$SU(2)\times SU(2)$	3	1	0	1	0	$-\frac{1}{2}$	−0.126	−0.061	0.187
2	$SU(3)\times SU(2)$	3	0	0	$\frac{2}{3}$	0	$-\frac{4}{3}$	−0.412	−0.382	0.794
3	$SU(3)\times SU(2)$	3	1	$\frac{1}{4}$	$\frac{2}{3}$	$-\frac{3}{8}$	$-\frac{4}{3}$	−0.412	−0.382	0.794
4	$SU(3)\times SU(2)$	3	2	$\frac{1}{2}$	$\frac{2}{3}$	$-\frac{3}{4}$	$-\frac{4}{3}$	−0.412	−0.382	0.794
5	$SU(3)\times SU(2)$	4	0	$\frac{1}{3}$	$\frac{2}{3}$	$-\frac{1}{2}$	−1	−0.288	−0.174	0.462
6	$SU(3)\times SU(2)$	4	1	$\frac{2}{3}$	$\frac{2}{3}$	−1	−1	−0.288	−0.174	0.462
7	$SU(6)\times SU(2)$	7	0	$\frac{7}{9}$	$\frac{1}{3}$	$-\frac{7}{3}$	$-\frac{3}{2}$	$-\frac{1}{2}$	$-\frac{1}{2}$	1
8	$SU(6)\times SU(2)$	7	1	$\frac{8}{9}$	$\frac{1}{3}$	$-\frac{8}{3}$	$-\frac{3}{2}$	$-\frac{1}{2}$	$-\frac{1}{2}$	1
9	$SU(8)\times SU(2)$	10	0	1	$\frac{1}{4}$	−4	$-\frac{3}{2}$	$-\frac{1}{2}$	$-\frac{1}{2}$	1

$$\gamma_\psi = -\frac{1}{2}, \qquad \gamma_\Psi = -\frac{1}{2}, \qquad \gamma_\chi = 1. \tag{39}$$

We conclude that the benchmark models are low-field-multiplicity realizations of asymptotic safety with phase diagrams as in Fig. 1. Most of them are nonperturbative with large $|\epsilon|$ and large anomalous dimensions, whose features are not captured reliably by a few leading orders of perturbation theory (Fig. 7). With increasing sizes of gauge group factors (N_1, N_2), many more solutions (N_F, N_Q) for the constraint (6) arise, and a fair fraction of these lead to an asymptotically safe fixed point within the UV conformal window (Fig. 2).

Finally, we discuss two benchmark models with $\epsilon = -\frac{3}{2}$ and maximal anomalous dimensions. These strongly coupled models are of the Leigh-Strassler type and narrowly outside the UV conformal window. The first one is model 8 with $SU(6)\times SU(2)$ gauge symmetry and $N_F = 7$, which differs from model 7 only in that $N_Q = 1$ instead of $N_Q = 0$, thus leading to a larger imbalance ($I = \frac{8}{9}$). In consequence, the ultraviolet fixed point of model 7 degenerates into a line of fixed points due to $\beta_2|_*$ vanishing identically at the gauge-Yukawa fixed point. The exactly marginal coupling α_2 becomes a free parameter and extends the fixed point into an infrared attractive line. The same phenomenon occurs for model 9, which has an $SU(8)\times SU(2)$ gauge symmetry with $N_F = 10$ and imbalance $I = 1$, situated at the lower-left corner of Fig. 2. Although interesting in their own right, models 8 and 9 no longer serve the purpose of ultraviolet fixed points. However, we stress that the method of a-maximization has been key in identifying fixed points with exactly marginal directions.

XI. CONCLUSIONS

We have shown, as a proof of principle, that interacting UV fixed points exist in strongly coupled quantum field theories including away from Veneziano (large-N) limits. Fixed point anomalous dimensions of matter fields can grow large, taking values in the entire range dictated by unitarity (26). Thereby, previously found perturbative fixed points [11] extend naturally into a nonperturbative conformal window (Fig. 6). Interestingly, a novel range of fixed points has become available, with no perturbative counterparts in a Veneziano limit (Fig. 7). We thus conclude that the nonperturbative "phase space" of fixed points is large and substantially larger than the one accessible at weak coupling. Further, all conformal fixed points (Fig. 2) are in accord with the a-theorem, bounds on central charges, Seiberg duality, and unitarity. We also found a manifold of Leigh-Strassler models arising at the sign-flip-controlling boundary of the conformal window, where theories display a line of IR fixed points generated by an exactly marginal gauge interaction (Fig. 4). It is understood that similar UV conformal windows, bounded by Leigh-Strassler manifolds, arise naturally in other semisimple gauge theories coupled to matter.

From the viewpoint of particle physics and model building, it is quite promising that fixed points persist at low field multiplicities (Table II), including with Standard-Model-like gauge groups. The next natural questions to ask are whether fixed points also arise in MSSM extensions [41] or in nonsupersymmetric settings at strong coupling. From the viewpoint of conformal field theory (CFT), it will be interesting to classify asymptotically safe supersymmetric theories more systematically and to extract CFT data or structure coefficients directly from the RG fixed points.

ACKNOWLEDGMENTS

The work of D. F. L. is supported by the Science and Technology Research Council (STFC) under the Consolidated Grant No. ST/T00102X/1.

[1] D. J. Gross and F. Wilczek, Ultraviolet Behavior of Non-Abelian Gauge Theories, Phys. Rev. Lett. **30**, 1343 (1973).
[2] H. D. Politzer, Reliable Perturbative Results for Strong Interactions?, Phys. Rev. Lett. **30**, 1346 (1973).
[3] S. Weinberg, Ultraviolet divergences in quantum theories of gravitation, in *General Relativity: An Einstein Centenary Survey*, edited by S. W. Hawking and W. Israel (Cambridge University Press, Cambridge, England, 1979), p. 790.
[4] D. Bailin and A. Love, Asymptotic near freedom, Nucl. Phys. **B75**, 159 (1974).
[5] D. F. Litim and F. Sannino, Asymptotic safety guaranteed, J. High Energy Phys. 12 (2014) 178.
[6] A. D. Bond and D. F. Litim, Price of Asymptotic Safety, Phys. Rev. Lett. **122**, 211601 (2019).
[7] A. D. Bond and D. F. Litim, Theorems for asymptotic safety of gauge theories, Eur. Phys. J. C **77**, 429 (2017).
[8] A. Bond and D. F. Litim, Interacting ultraviolet completions of four-dimensional gauge theories, Proc. Sci. LATTICE2016 (**2017**) 208.
[9] A. D. Bond, D. F. Litim, and T. Steudtner, Asymptotic safety with Majorana fermions and new large N equivalences, Phys. Rev. D **101**, 045006 (2020).
[10] A. D. Bond and D. F. Litim, More asymptotic safety guaranteed, Phys. Rev. D **97**, 085008 (2018).
[11] A. D. Bond and D. F. Litim, companion paper, Asymptotic Safety Guaranteed in Supersymmetry, Phys. Rev. Lett. **119**, 211601 (2017).
[12] A. D. Bond, G. Hiller, K. Kowalska, and D. F. Litim, Directions for model building from asymptotic safety, J. High Energy Phys. 08 (2017) 004.
[13] K. Kowalska, A. Bond, G. Hiller, and D. Litim, Towards an asymptotically safe completion of the standard model, *Proc. Sci.* EPS-HEP2017 (2017) 542.
[14] G. Hiller, C. Hormigos-Feliu, D. F. Litim, and T. Steudtner, Asymptotically safe extensions of the standard model with flavour phenomenology, in *Proceedings of the 54th Rencontres de Moriond on Electroweak Interactions and Unified Theories*, edited by E. Auge, J. Dumarchez, and J. Tran Thanh Van (2019), pp. 415–418, arXiv:1905.11020.
[15] G. Hiller, C. Hormigos-Feliu, D. F. Litim, and T. Steudtner, Anomalous magnetic moments from asymptotic safety, Phys. Rev. D **102**, 071901 (2020).
[16] G. Hiller, C. Hormigos-Feliu, D. F. Litim, and T. Steudtner, Model building from asymptotic safety with Higgs and flavor portals, Phys. Rev. D **102**, 095023 (2020).
[17] S. Bißmann, G. Hiller, C. Hormigos-Feliu, and D. F. Litim, Multi-lepton signatures of vector-like leptons with flavor, Eur. Phys. J. C **81**, 101 (2021).
[18] R. Bause, G. Hiller, T. Höhne, D. F. Litim, and T. Steudtner, B-anomalies from flavorful $U(1)'$ extensions, safely, Eur. Phys. J. C **82**, 42 (2022).
[19] D. F. Litim, M. Mojaza, and F. Sannino, Vacuum stability of asymptotically safe gauge-Yukawa theories, J. High Energy Phys. 01 (2016) 081.
[20] T. Buyukbese and D. F. Litim, Asymptotic safety of gauge theories beyond marginal interactions, Proc. Sci. LATTICE2016 (**2017**) 233.
[21] S. Abel and F. Sannino, Radiative symmetry breaking from interacting UV fixed points, Phys. Rev. D **96**, 056028 (2017).
[22] A. D. Bond, D. F. Litim, G. Medina Vazquez, and T. Steudtner, UV conformal window for asymptotic safety, Phys. Rev. D **97**, 036019 (2018).
[23] A. D. Bond, D. F. Litim, and G. M. Vazquez, Conformal windows beyond asymptotic freedom, Phys. Rev. D **104**, 105002 (2021).
[24] V. Novikov, M. A. Shifman, A. Vainshtein, and V. I. Zakharov, Exact Gell-Mann-Low function of supersymmetric Yang-Mills theories from instanton calculus, Nucl. Phys. **B229**, 381 (1983).
[25] V. Novikov, M. A. Shifman, A. Vainshtein, and V. I. Zakharov, The beta function in supersymmetric gauge theories instantons versus traditional approach, Sov. J. Nucl. Phys. **43**, 294 (1986).
[26] K. A. Intriligator and B. Wecht, The exact superconformal R symmetry maximizes a, Nucl. Phys. **B667**, 183 (2003).
[27] G. Mack, All unitary ray representations of the conformal group SU(2,2) with positive energy, Commun. Math. Phys. **55**, 1 (1977).
[28] K. Stepanyantz, The all-loop perturbative derivation of the NSVZ β-function and the NSVZ scheme in the non-Abelian case by summing singular contributions, Eur. Phys. J. C **80**, 911 (2020).
[29] D. Korneev, D. Plotnikov, K. Stepanyantz, and N. Tereshina, The NSVZ relations for $\mathcal{N} = 1$ supersymmetric theories with multiple gauge couplings, J. High Energy Phys. 10 (2021) 046.
[30] D. Kutasov and A. Schwimmer, Lagrange multipliers and couplings in supersymmetric field theory, Nucl. Phys. **B702**, 369 (2004).
[31] R. G. Leigh and M. J. Strassler, Exactly marginal operators and duality in four-dimensional $N = 1$ supersymmetric gauge theory, Nucl. Phys. **B447**, 95 (1995).
[32] D. Anselmi, D. Freedman, M. T. Grisaru, and A. Johansen, Nonperturbative formulas for central functions of supersymmetric gauge theories, Nucl. Phys. **B526**, 543 (1998).
[33] D. Anselmi, J. Erlich, D. Z. Freedman, and A. A. Johansen, Positivity constraints on anomalies in supersymmetric gauge theories, Phys. Rev. D **57**, 7570 (1998).
[34] D. M. Hofman and J. Maldacena, Conformal collider physics: Energy and charge correlations, J. High Energy Phys. 05 (2008) 012.
[35] Z. Komargodski and A. Schwimmer, On renormalization group flows in four dimensions, J. High Energy Phys. 12 (2011) 099.
[36] Z. Komargodski, The constraints of conformal symmetry on RG flows, J. High Energy Phys. 07 (2012) 069.
[37] N. Seiberg, Electric-magnetic duality in supersymmetric non-Abelian gauge theories, Nucl. Phys. **B435**, 129 (1995).
[38] E. Barnes, K. A. Intriligator, B. Wecht, and J. Wright, $N = 1$ RG flows, product groups, and a-maximization, Nucl. Phys. **B716**, 33 (2005).
[39] M. B. Einhorn and D. R. T. Jones, Scale fixing by dimensional transmutation: Supersymmetric unified models and the renormalization group, Nucl. Phys. **B211**, 29 (1983).
[40] M. E. Machacek and M. T. Vaughn, Two loop renormalization group equations in a general quantum field theory. 1. Wave function renormalization, Nucl. Phys. **B222**, 83 (1983).
[41] G. Hiller, D. F. Litim, and K. Moch, Fixed points in supersymmetric extensions of the standard model, arXiv:2202.01264.